Available online at www.sciencedirect.com
ScienceDirect
Precambrian Research 149 (2006) 77–98
Precambrian Research
www.elsevier.com/locate/precamres

# Growth-fault structure and stratigraphic architecture of the Buck Ridge volcano-sedimentary complex, upper Hooggenoeg Formation, Barberton Greenstone Belt, South Africa

Sjoukje T. de Vries [a,*], Wouter Nijman [a], Richard A. Armstrong [b]

[a] *Department of Earth Sciences, Utrecht University, Budapestlaan 4, 3584 CD Utrecht, The Netherlands*
[b] *Research School of Earth Sciences, The Australian National University (ANU), Canberra, ACT 0200, Australia*

Received 28 January 2005; received in revised form 11 April 2006; accepted 22 April 2006

**Abstract**

The ~3.45–3.42 Ga Buck Ridge volcano-sedimentary complex (BR-vsc) forms the uppermost part of the Hooggenoeg Formation, in the early Archaean Onverwacht Group of the Barberton Greenstone Belt, South Africa. The complex consists mainly of massive and pillowed basalts and felsic, quartz-plagioclase porphyritic rocks, which are capped by pervasively silicified sedimentary rocks. Deposition of the felsic extrusive and (volcani-)clastic sedimentary rocks occurred in shallow water to emersion, during an extensional tectonic regime. The extensional regime is expressed by a number of listric normal faults that transect the entire ~2 km thick complex. The syndepositional (i.e. growth fault) character of the faults is indicated by variations in thickness and facies of rock units across the faults, and by systematic rotation of the fault blocks. Broadly contemporaneous with the faulting, felsic rocks intruded the complex into the highest levels. The geometry of these intrusive bodies was controlled by the major growth faults. Extension also created space for the intrusion of approximately bedding-perpendicular felsic and mafic dykes, and black chert veins. The new field observations and U–Pb zircon SHRIMP data have pinned the timing of events during and after deposition of the BR-vsc. The growth-fault model accounts well for previously unexplained structural observations that include both extensional and compressional features. Recognition of an early extensional phase of deformation demonstrates further similarities between the tectonic histories of the Barberton Greenstone Belt and the greenstone belts of the east Pilbara in Australia.


*Keywords:* Early Archaean; Early extension; Syndepositional normal faulting; Geochronology; Onverwacht Group; Barberton Greenstone Belt

## 1. Introduction

Sedimentary rocks of the ~3.42 Ga Buck Ridge Chert (BRC, also referred to as Buck Reef Chert; Lowe and Byerly, 1999a) of the upper Hooggenoeg Formation are amongst the oldest preserved clastic deposits in the Barberton Greenstone Belt (South Africa). The sedimentary rocks are well preserved and have experienced little deformation. Therefore, they form a good target for early Archaean basin studies. Knowledge of the tectonic regime during which these basins were formed, and hence the timing of the earliest phase of crustal deformation, is essential. Despite the fact that the Barberton Greenstone Belt has been intensively studied, the tectonic regime during deposition of the upper Hooggenoeg Formation is still not well known. Extensional faults (Viljoen and Viljoen, 1969; de Wit, 1982, 1986; Lowe and Fisher Worrell, 1999) as well as compressive features (de Wit, 1982, 1983; de Wit et al., 1987a; Lowe et al., 1985, 1999) have been reported. However, it

* Corresponding author. Tel.: +61 2 6283 4800.
*E-mail address:* stdevries@geo.uu.nl (S.T. de Vries).

0301-9268/$ – see front matter © 2006 Elsevier B.V. All rights reserved.
doi:10.1016/j.precamres.2006.04.005

remains unclear whether basin formation was controlled by an extensional or a compressive tectonic regime, and what the temporal relationship between these tectonic regimes was. Some conspicuous features in the upper Hooggenoeg Formation, such as the Geluk disturbed zone, described by Lowe et al. (1985, 1999) as a zone of rotated and overturned blocks, remained largely unexplained, and were not attributed to a particular tectonic regime. We present new field and geochronological data that allow for a more detailed interpretation of the structural control during deposition of the upper Hooggenoeg Formation. In this study it was found that observations of syndepositional deformation provide the most useful clues about the structural control in this basin. Attention will also be paid to the structure of the area immediately to the north of the BRC, because the connection between the BRC and the overlying stratigraphic units is relatively poorly known.

## 2. Geological framework

### 2.1. Stratigraphy

Stratigraphically, rocks of the Archaean Barberton Greenstone Belt belong to the Swaziland Supergroup, which is divided into the dominantly volcanic Onverwacht Group and the overlying sedimentary Fig Tree and Moodies Groups. The intact stratigraphic section of the Onverwacht Group consists of four units: the ~3.48–3.27 Ga Komati, Hooggenoeg, Kromberg, and Mendon Formations (e.g. Viljoen and Viljoen, 1969; Armstrong et al., 1990; Kröner et al., 1991; Kamo and Davis, 1994; Byerly et al., 1996; Lowe and Byerly, 1999b).

The Hooggenoeg Formation dominantly consists of mafic and ultramafic rocks that occasionally include thin layers of silicified sedimentary rocks. The uppermost part of the formation is made up of a 1–2 km thick succession of basalt with several layers of felsic volcanic and volcaniclastic rocks, and a minor amount of felsic intrusive rocks (e.g. Viljoen and Viljoen, 1969; de Wit, 1982; Lowe et al., 1985; de Wit et al., 1987a; Lowe and Byerly, 1999b). The extrusive felsic rocks are capped by up to 570 m of sedimentary rocks of the BRC. The Kromberg and Mendon Formations consist of mafic to ultramafic volcanic and volcaniclastic rocks, and include thin layers of silicified sedimentary rocks (e.g. Viljoen and Viljoen, 1969; Lowe and Byerly, 1999b).

Opinions differ about whether the BRC belongs to the Hooggenoeg Formation or to the Kromberg Formation. The BRC was originally placed at the top of the Hooggenoeg Formation (Viljoen and Viljoen, 1969). This interpretation was widely adopted until Byerly et al. (1996) re-interpreted the BRC as the basal unit of the Kromberg Formation. These authors regarded the BRC to be the lateral equivalent of several thin cherts in the Kromberg Formation on the southern limb of the Onverwacht Bend. Since then, there has been a debate about which formation the BRC should be assigned to. Brandl and de Wit (1997) regard it as the uppermost unit of the Hooggenoeg Formation, whereas Lowe and Byerly (1999a) continued to interpret it as the base of the Kromberg Formation. In our study area, the contact of the BRC with the underlying layers of the Hooggenoeg Formation is generally transitional (cf. Viljoen and Viljoen, 1969; Lowe and Fisher Worrell, 1999). Local unconformities are present, but there is no regional unconformity at the base of the BRC. The transitional contact of the BRC with the underlying rocks, and the fact that further west the BRC splits up in an alternation of chert, shale and Hooggenoeg Formation basalt, indicate that the BRC should be regarded as part of the latter formation (cf. Viljoen and Viljoen, 1969). For the assemblage of interrelated basalts, felsic volcanic rocks and intercalated cherts in the upper part of the Hooggenoeg Formation a new term is introduced: the Buck Ridge volcano-sedimentary complex (BR-vsc). The BRC forms the silicified, uppermost part of this complex. The base of the BRC is taken where the uppermost felsic volcanic rocks of the BR-vsc grade into pervasively silicified, black-and-white-banded sedimentary rocks.

### 2.2. Structural setting

The rock succession of the Barberton Greenstone Belt has undergone several phases of intense folding and faulting, which have resulted in a generally vertical to subvertical orientation of the bedding. Main phases of deformation that led to the folding and thrusting of the greenstone belt succession are interpreted to be D1 and D2, at ~3445 and 3230 Ma (Table 1). Deformation phases D3 and D4 led to further folding and faulting. During D3, the entire southern part of the greenstone belt was folded into the steeply east-plunging Onverwacht Bend (Fig. 1). The study area is located on the northern limb of this antiform, where the overall younging is to the north (dating by e.g. Armstrong et al., 1990; Kröner et al., 1991; Kamo and Davis, 1994; Byerly et al., 1996).

There has been debate about the stratigraphic continuity in the study area on a smaller scale. Viljoen and Viljoen (1969) provided one of the first maps and a systematic description of the stratigraphic succession of the area (Fig. 2a). They regarded the Hooggenoeg Formation as an essentially continuous, north-younging

Table 1
Current deformation scheme for the southern part of the Barberton Greenstone Belt

| Phase | Nature | Timing | Description | References |
|---|---|---|---|---|
| D0 | Extension | ? ~3486 Ma | Normal faulting, decollement | de Wit (1986) |
| | | ~3.48–3.46 Ga | Carbonate extension veins, shearing | Zegers et al. (1998) and references therein |
| D1 | Compression | 3445–3416 Ma | Recumbent nappes, downward facing sequences | de Ronde and de Wit (1994) |
| D2 | Compression | 3229–3227 Ma | SE to NW thrusting, tight isoclinal folding | de Ronde and de Wit (1994) |
| D3 | Compression | 3226–3084 Ma | NW vergent thrusting, folding | de Ronde and de Wit (1994) |
| D4 | Extension | <3084 Ma | Folding, strike-slip faulting | de Ronde and de Wit (1994) |

stratigraphic succession. Williams and Furnell (1979) suggested the possibility of tectonic discontinuities in the upper Hooggenoeg Formation. De Wit (1982, 1983), de Wit et al. (1987a) and Lowe et al. (1985, 1999) observed deformation in the upper Hooggenoeg Formation that included folding, shearing and rotation of lithological packages. The exact nature and timing of the tectonic regime that caused the deformation in the upper Hooggenoeg Formation are also debated. Early extensional deformation (D0) in the southern Barberton Greenstone Belt has also been suggested (de Wit, 1982, 1986; Zegers et al., 1998), but evidence remained sparse and the timing not well constrained. Generally, compressive deformation is interpreted to have dominated in the southern Barberton Greenstone Belt during deposition of the upper Hooggenoeg Formation (Table 1 and references therein). Lowe et al. (1999) proposed a deformation scheme in which the first phase of deformation is expressed by a zone of shearing and block rotation that was observed in the upper Hooggenoeg Formation. They suggested that the lower contact of the zone might have formed as a south-dipping thrust or reverse fault. However, the observations were not placed in a regional framework or attributed to a particular tectonic regime.

## 3. New observations on the Buck Ridge volcano-sedimentary complex

### 3.1. General remarks

Mapping was accomplished on a 1:6000 scale, and was based on extensive field observations, including detailed sedimentary logging. In addition, normal aerial photographs and low-level oblique aerial photographs taken from a microlight-plane were used. Field observations were complemented with petrographical and geochronological analyses. Dating of zircons from four samples was carried out on the SHRIMP-RG of the Research School for Earth Sciences at the Australian National University (see appendix for analytical details).

The broadly east–west striking rock succession in the study area is overall younging to the north, and dips are near-vertical to steeply overturned. Therefore, the

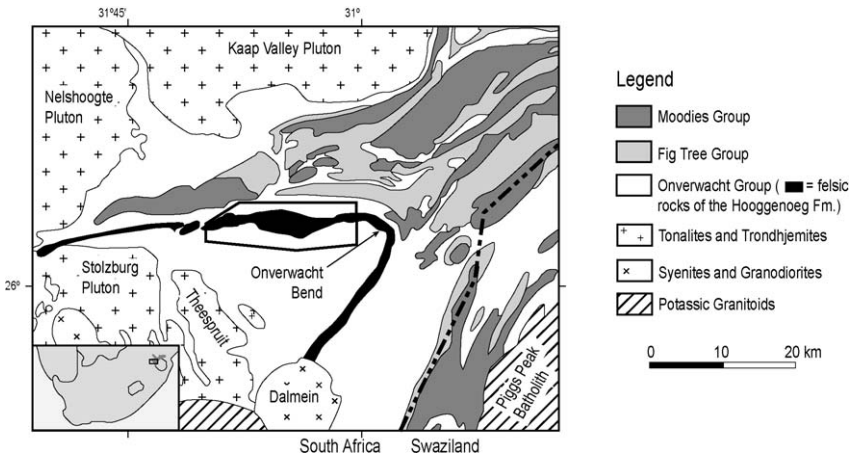


Fig. 1. Schematic geological map of the southern part of the Barberton Greenstone Belt with surrounding granitoid complexes and its location in South Africa (modified after de Ronde and de Wit, 1994; Kisters et al., 2003). Study area indicated with a rectangle.

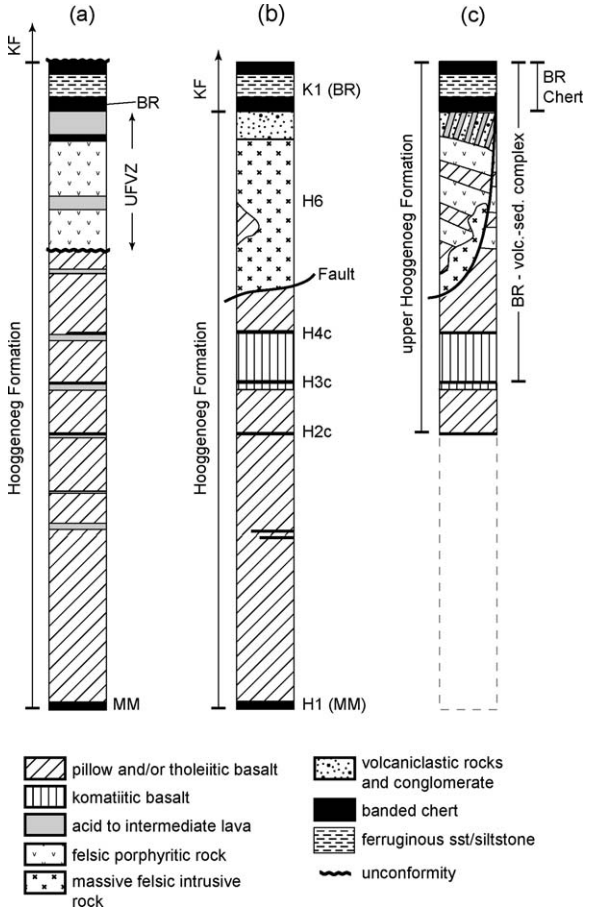


Fig. 2. Simplified stratigraphic columns of the Hooggenoeg Formation on the northern limb of the Onverwacht Bend. KF, Kromberg Formation; UFVZ, upper felsic volcanic zone; BR, Buck Ridge (or Reef); MM, Middle Marker. (a) Based on the map and description of Viljoen and Viljoen (1969); (b) modified after Lowe and Byerly (1999a); (c) terminology used in this article. 'b' and 'c' are from approximately the same location; 'a' was taken slightly more west. Due to syndepositional faulting, both thickness and composition of the felsic volcaniclastic succession vary considerably along strike (see text and Fig. 3). This partly explains the relatively thin felsic zone and the absence of volcaniclastic rocks in 'a'.

map of the study area (Fig. 3) can be read as a cross-section through the BR-vsc. Fig. 3 shows that the BR-vsc is a ~2 km thick part of the Hooggenoeg Formation, which is characterised by intraformational, clockwise strike deviations of up to 60° from the overall east–west strike of the succession. The strike deviations end against northeast-trending faults, which are restricted to the stratigraphic interval of the BR-vsc. The array of NE-trending faults extends over a distance of at least 15 km, along almost the entire length of the northern limb of the Onverwacht Bend. The BR-vsc is bounded by a stack of approximately bedding parallel shear zones on the lower (i.e. southern) side, and by the east–west striking uppermost units of the BRC on the northern side.

In the now forested area north of the Buck Ridge, black-and-white-banded chert of the top of the north-younging BRC can be traced via low-angle, east-dipping outcrops and block alignments (loc. HV98-261; Figs. 3 and 4) into the south-facing northern limb of what appears to be a major synclinal structure, the Granville Syncline (*new name*). Towards the west, this syncline is obliquely truncated by the Saddleback-Inyoka Fault (a suture that separates two major structural domains of the Barberton Greenstone Belt, cf. de Ronde and de Wit, 1994; Brandl and de Wit, 1997; de Ronde and Kamo, 2000).

### 3.2. Stratigraphy and geochronology

#### 3.2.1. Volcanic and sedimentary rocks of the BR-vsc

The BR-vsc forms a broadly continuous stratigraphic succession in the uppermost part of the Hooggenoeg Formation. The lower part of the BR-vsc consists predominantly of poorly exposed, massive and pillowed basalts, minor komatiites and ~2–8 m thick layers of silicified sedimentary rocks. The thickness of the basalt succession varies, but it makes up about 60% of the BR-vsc. The intercalated silicified sedimentary rocks show well-preserved cross-bedding and grading, providing indicators for the direction of younging (which is generally to the north). Stratigraphically upward, felsic layers are intercalated with, and gradually become dominant over, the basalts (Figs. 2c and 3). The felsic rocks are porphyritic and contain quartz and altered plagioclase phenocrysts in a cryptocrystalline groundmass (for additional petrographic details on the igneous rocks, see Table 2). In places, the porphyritic rocks are flow-banded or show columnar jointing. A sample of such a flow-banded porphyritic rock from just below the BRC, in the footwall of one of the major normal faults (loc. LV01-23) was dated at 3451 ± 5 Ma (U–Pb SHRIMP dating, Fig. 5a and Appendix A). Towards the top, volcaniclastic rocks are intercalated with the porphyritic rocks. In the eastern part of the area, where the Mtsoli River cuts the upper part of the BR-vsc, the volcaniclastic rocks are coarse-grained and include agglomerate (cf. de Wit, 1983) and, at the base, polymictic pebble-cobble conglomerate. Towards the west they generally consist of finer-grained deposits, tuff and, rarely, layers containing accretionary lapilli. The combined thickness of the felsic porphyritic and volcaniclastic rocks (shown as one lithology in Fig. 3, thickness excluding sills) varies along strike in the study area. It attains maximal thicknesses of 600–730 m immediately to the west of the NE-trending

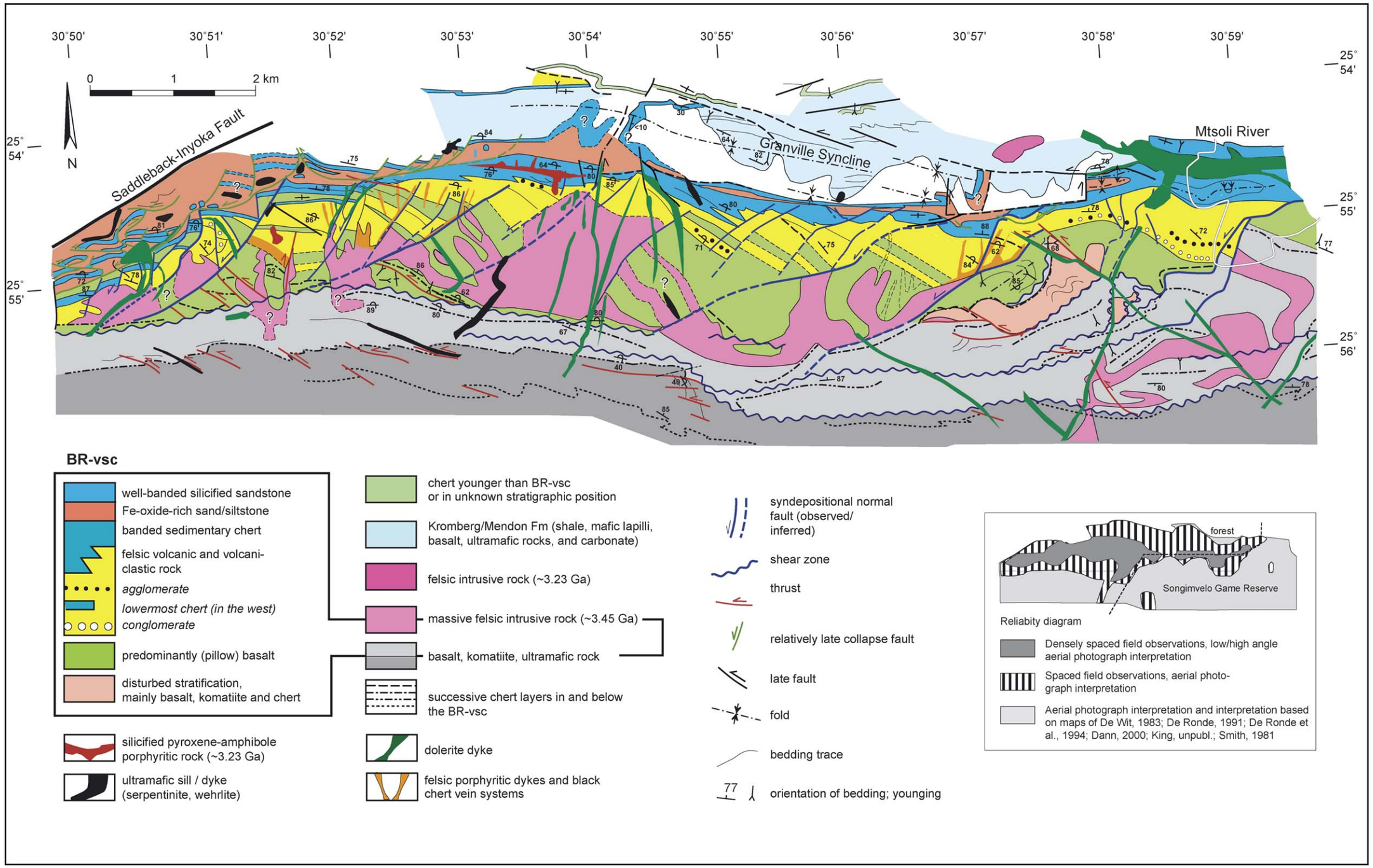


Fig. 3. Geological map of the study area (location indicated in Fig. 1). The orientation of bedding is near-vertical, therefore the map also represents a cross-section through the upper part of the Hooggenoeg Formation. References cited in reliability diagram (inset): de Wit, 1983; de Ronde, 1991; de Ronde et al., 1994; Dann, 2000; King, unpubl.; Smith, 1981.

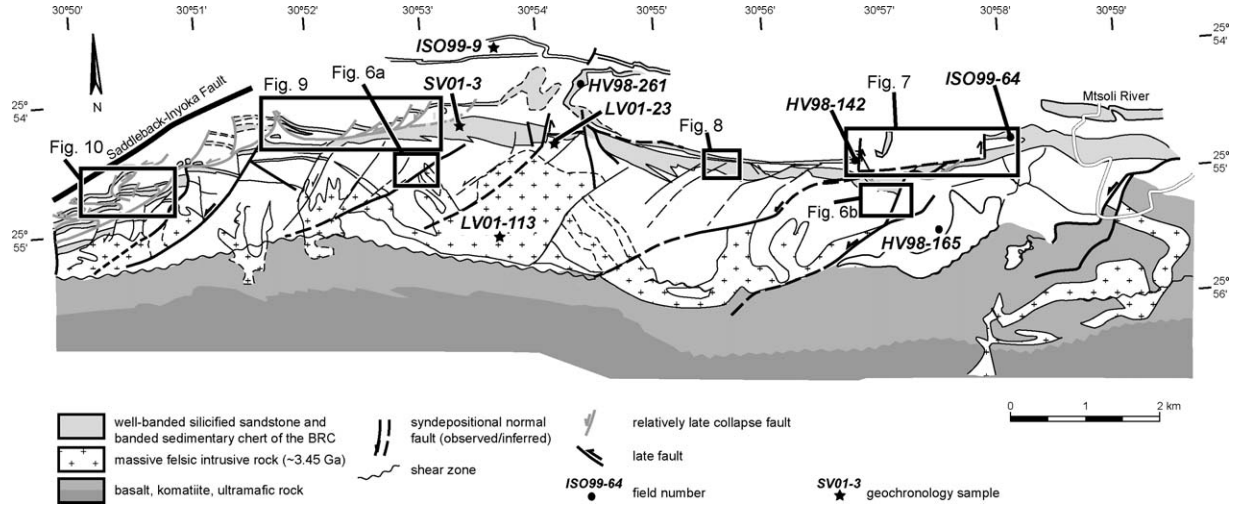


Fig. 4. Reference map (after Fig. 3), indicating location of figures, field numbers, and geochronology samples mentioned in the text.

faults, and minimal thicknesses of 100–430 m on their eastern sides. In the western part of the area (pillow), basalts and sedimentary chert layers are intercalated with the uppermost felsic volcanic rocks.

The sedimentary top of the BR-vsc, the Buck Ridge Chert (BRC), consists from old to young of partly silicified volcaniclastic rocks, a thick interval of banded sedimentary chert, an iron-oxide-rich sandstone–siltstone

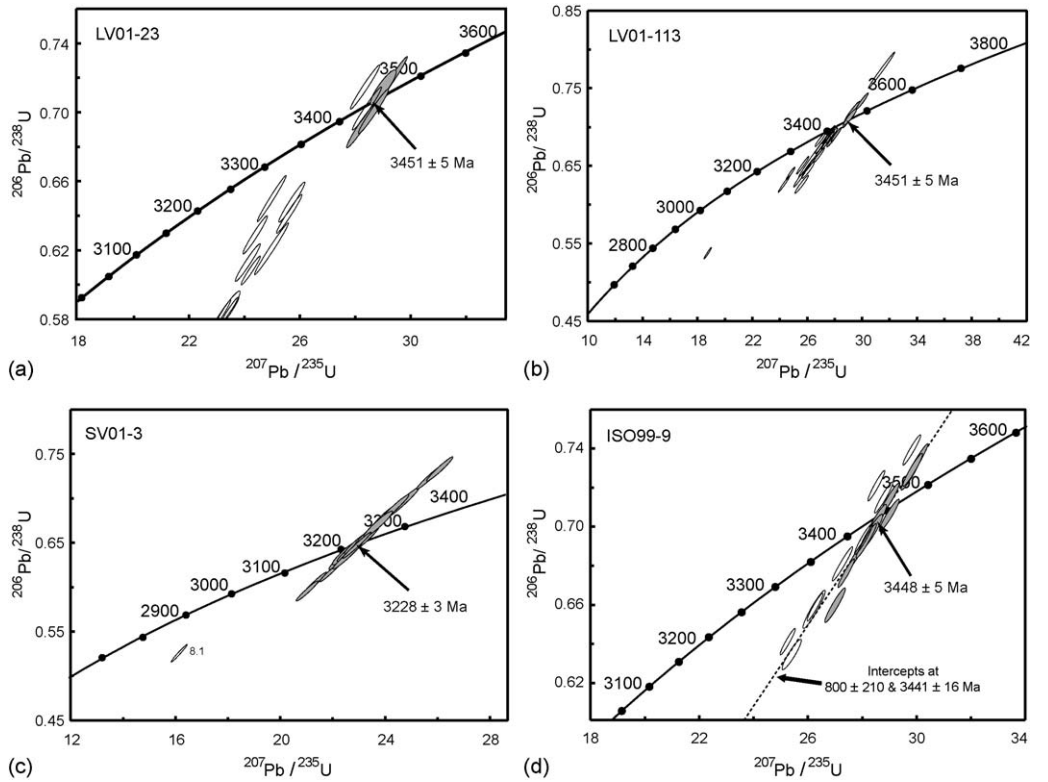


Fig. 5. Concordia diagrams of U–Pb data for samples dated with the SHRIMP-RG of the Research School for Earth Sciences at the Australian National University in Canberra. Data in filled error ellipses were used to calculate the mean $^{207}Pb/^{206}Pb$ age. Data point error ellipses are 68.3% confidence. Details on the analytical technique and the results for the individual samples are given in Appendix A.

Table 2
Additional details on the main in- and extrusive igneous rocks of the BR-vsc, general characteristics described in Section 3.2

| | Groundmass | Minerals | Age (Ma) |
|---|---|---|---|
| Felsic rocks north of the Buck Ridge Chert (dating sample ISO99-9) | Cryptocrystalline, dominantly consisting of microquartz and sericite. | Phenocrysts: quartz: ~0.02–0.6 mm large, subhedral. Rectangular ghost minerals: ~0.2–1.8 mm large, now completely consisting of sericite. Outlines of these ghost minerals are still very rectangular (probably originally plagioclase). | 3448 ± 5 |
| Felsic extrusive rocks (incl. dating sample LV01-23) | Cryptocrystalline, consisting of microquartz and sericite. Percentage of groundmass: ~65–80%. | Phenocrysts: homogeneously distributed. Quartz: euhedral, 0.2–3 mm large. Plagioclase: lath-shaped, ~1 mm, locally reaching up to 4 mm. Plagioclase often altered to sericite. | 3451 ± 5 |
| Main felsic intrusive rocks (incl. dating sample LV01-113) | No groundmass in core of intrusion, small percentage (up to 20%) towards the rims. | Plagioclase: 1–2 mm, make up 65–75% of the rock volume. Quartz: average size 0.5 mm (max. 2.5 mm), make up 15–25% of the total volume. Chlorite is present as a secondary phase. | 3451 ± 5 |
| Minor felsic intrusions | Finely crystalline, 50% of the total rock volume. | Plagioclase: rectangular, 0.5–3 mm large. Generally altered to sericite, but simple and multiple twinning have occasionally been preserved. Quartz present. | Dating unsuccessful |
| Altered pyroxene-amphibole-bearing rocks (incl. dating sample SV01-3) | Fine-grained, constitutes 25–75% of the total rock volume. | Phenocrysts: homogeneously distributed. Dark, thin, needle-shaped laths: avg. length 0.6 mm, cryptocrystalline. More equi-dimensional laths: up to 2.2 mm, less abundant than the dark laths. Often twinned (i.e. presumably plagioclase). Altered, brown, hexagonal minerals: 0.5–3 mm, euhedral to subhedral, cryptocrystalline (presumably originally pyroxenes or amphiboles). | 3228 ± 3 |

interval with dispersed breccia bodies and a well-banded silicified sandstone. The contact between the silicified volcaniclastic deposits and the underlying felsic volcanic and volcaniclastic rocks is transitional (cf. Viljoen and Viljoen, 1969; Lowe and Fisher Worrell, 1999). Locally, the volcaniclastic interval is very thin or not present at all, and the banded sedimentary cherts immediately overlie quartz-plagioclase porphyritic lavas. The lower part of the BRC, particularly the silicified volcaniclastic rocks and the banded sedimentary chert, show similar thickness variations (e.g. from 100 to 530 m in the central part of the map area) across the NE-trending faults as the underlying felsic volcanic rocks. Upward in the section, the thickness variation diminishes, and the well-banded silicified sandstone at the top of the succession has a relatively constant thickness of several tens of metres.

### 3.2.2. Intrusive rocks

Several types and generations of igneous rock have intruded the BR-vsc.

*3.2.2.1. Massive felsic intrusions.* Massive, predominantly quartz-plagioclase-bearing felsic intrusive bodies (Fig. 3) occur with a regular spacing of ~2–4 km in the lower part of the BR-vsc. The felsic bodies are asymmetric, with NE–SW-oriented long axes, smooth contacts on the southeastern side, and irregular northwestward contacts. The spacing of the intrusions roughly corresponds with the spacing of the major NE-trending faults that cut the BR-vsc. The smooth southeastern sides of the intrusions line up with the faults. Stratigraphically, the bases of the felsic intrusions occur at approximately 1.7–2.6 km below the top of the BR-vsc, just above or within the zone of bedding-parallel shear zones (Fig. 3). U–Pb SHRIMP dating of a sample from the core of one of the massive intrusions in the central part of the map area (loc. LV01-113) yielded an age of 3451 ± 5 Ma (Fig. 5b and Appendix A).

*3.2.2.2. Felsic sills.* From the northwestern sides of the massive felsic intrusions, felsic porphyritic sills project into the bimodal volcanic succession of the BR-vsc.

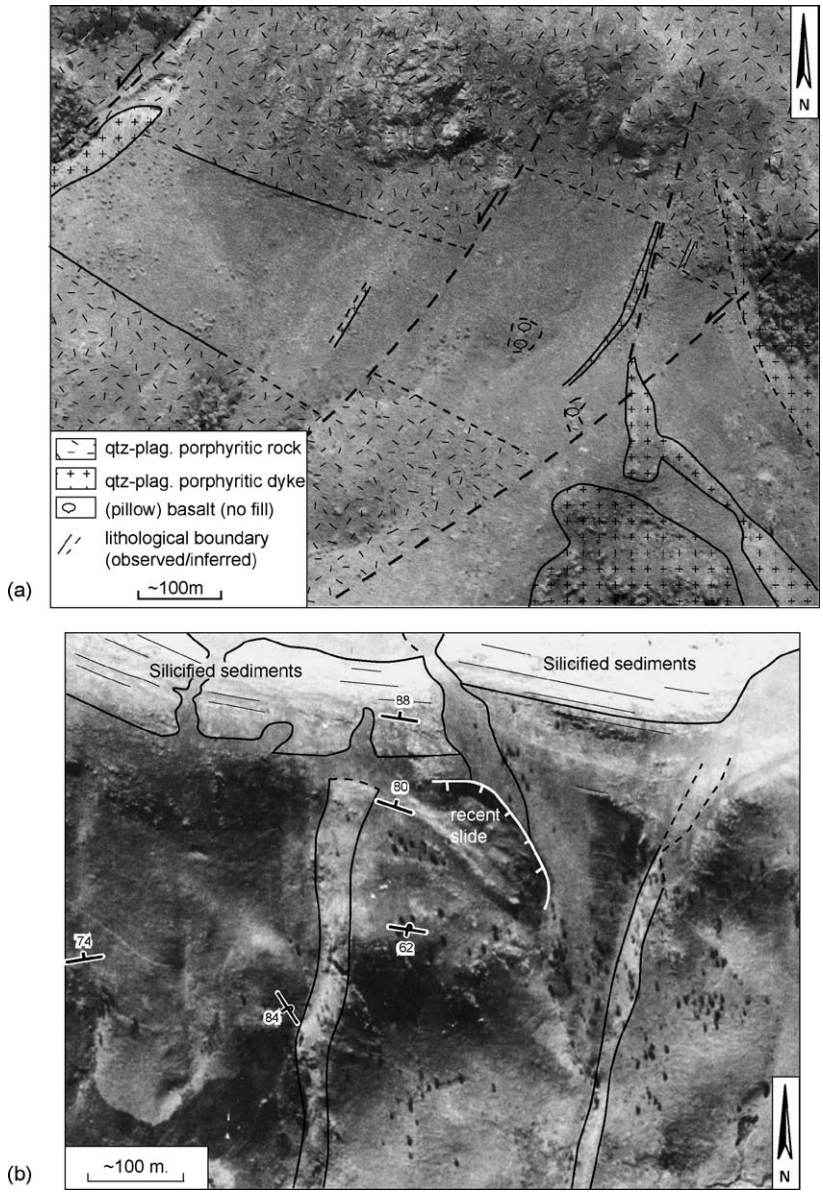


Fig. 6. (a) Quartz-plagioclase porphyritic dykes cutting a poorly exposed pillow basalt interval. (b) Pale, approximately N–S-oriented structures in a poorly exposed felsic volcanic rock interval overlain by silicified sedimentary rocks of the Buck Ridge Chert. Thin lines in the silicified sedimentary rocks represent orientation of bedding. Locations are indicated in Fig. 4. Aerial photographs: Chief Directorate of Surveys and Mapping, South Africa.

These sills consist of porphyritic felsic rocks with small amounts (up to 50% of the total rock volume) of groundmass. Bedding-parallel quartz-plagioclase porphyritic rocks without flow banding or columnar jointing also occur in the felsic volcanic succession immediately below the BRC.

*3.2.2.3. Felsic porphyritic dykes.* In several places, felsic dykes cut the bimodal volcanic succession at high angles (Fig. 6). They often have a distinct light weathering colour, and traverse both poorly exposed pillow basalt intervals (Fig. 6a) and felsic volcanic host rocks (Fig. 6b). The dykes consist of quartz-plagioclase porphyritic rocks, and generally have a fine-grained, almost glassy groundmass. The porphyritic rocks were locally brecciated and subsequently cemented with chert or quartz. The dykes terminate in the highest bedding-parallel felsic units of the upper Hooggenoeg Formation. Metres-wide black chert veins occur in the vicinity and have approximately the same (bedding-perpendicular)

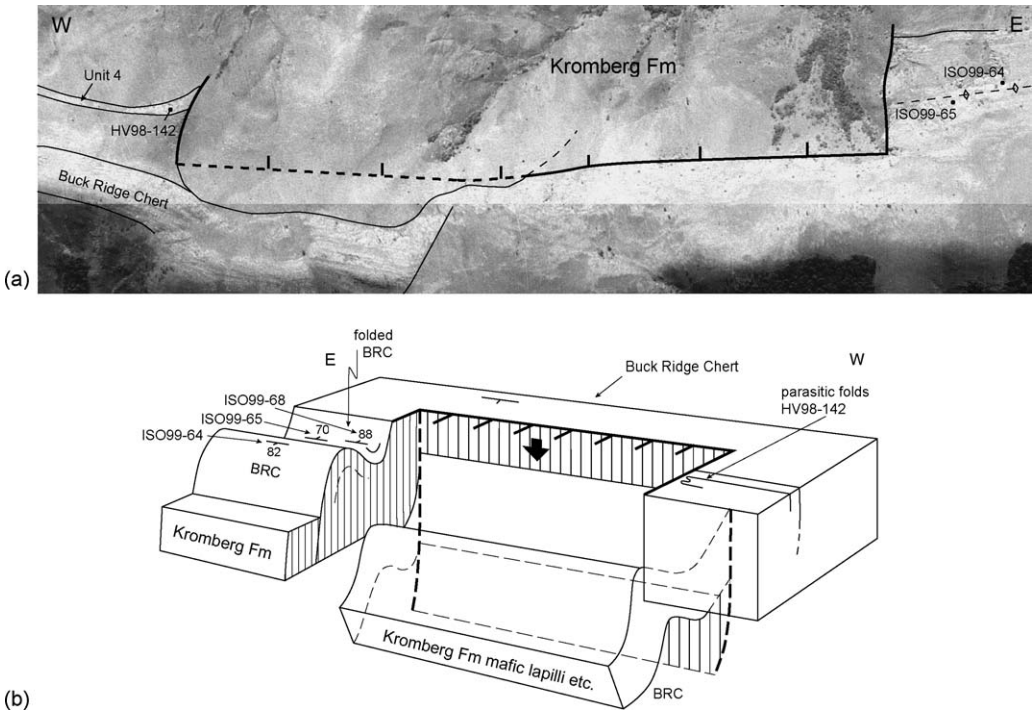


Fig. 7. (a) Aerial photograph (Chief Directorate of Surveys and Mapping, South Africa) of the area (location indicated in Fig. 4) where, locally, the top of the BR-vsc is missing. (b) Sketch model of how local folding and faulting of the upper part of the BR-vsc may have resulted in juxtaposition of BR-vsc sedimentary rocks and Kromberg Formation mafic deposits in the area shown in 'a'.

orientation. With depth, the felsic dykes appear to merge with the main felsic intrusions (Fig. 3).

*3.2.2.4. Mafic intrusions.* Mafic intrusions in the BR-vsc include silicified dolerite dykes, which have approximately the same orientation as the quartz-plagioclase porphyritic dykes. Part of these dolerite dykes end in a basalt interval in the uppermost part of the BR-vsc. Other, mostly less-weathered dolerite dykes cut through the entire BR-vsc. The uppermost part of the BR-vsc has been intruded by (now largely silicified) porphyritic pyroxene-amphibole-bearing rocks. U–Pb zircon dating of these intrusions yielded an age of $3228 \pm 3$ Ma (sample SV01-03, Fig. 5c and Appendix A). Furthermore, the BR-vsc is traversed by relatively fresh, coarse-grained ultramafic dykes (including wehrlites, described by Dann, 2000), and by very fine-grained and in places completely altered mafic dykes.

### *3.2.3. Rock units of the core and northern limb of the Granville Syncline*

The rocks of the core and northern limb of the Granville Syncline are exposed in road cuts and isolated outcrops. They include mafic and ultramafic intrusive rocks, basalts, tuffs, black-and-white-banded chert, cross-bedded, carbonate rich sandstones, and shales. Sedimentologically, the banded cherts resemble the well banded, in places cross-laminated silicified sandstone of the uppermost BRC. Westward, a succession of black-and-white-banded chert and felsic porphyry occurs along the northern synclinal limb (loc. ISO99-9; Figs. 3 and 4). Quartz-plagioclase porphyritic rocks at this location mineralogically and texturally strongly resemble the felsic porphyritic rocks just below the BRC (e.g. loc. LV01-23). U–Pb dating of the felsic porphyritic rock yielded an age of $3448 \pm 5$ Ma (details in Fig. 5d and Appendix A).

Cherts along the northern limb and rocks in the core of the Granville Syncline between 30°55′E and 30°58′E are considered to belong to the Kromberg and Mendon Formations (e.g. Viljoen and Viljoen, 1969; de Wit et al., 1987a; Kamo and Davis, 1994; Lowe and Byerly, 1999b).

Between ~30°57′E and 30°58′E (Figs. 3 and 7), part of the BRC is reported to be directly juxtaposed with mafic lapilli tuffs attributed to the Kromberg Formation (Ransom et al., 1999).

## *3.3. Structure*

Analysis of the *first, syndepositional* phase of deformation is quite different from the analysis of phases of

deformation that took place at greater depth. First, many structural features that characterise more ductile phases of deformation, such as lineations, schistosities or foliations, generally do not form in the uppermost part of the crust, because the overburden at the time of the first deformation is too low. Second, the preservation of foliations, fractures and tension gashes at shallow crustal levels is often particularly poor because of overprinting and alteration by later phases of fluid motion, including percolating water during phases of emersion. The analysis of the first phase of deformation therefore often depends on other diagnostic criteria than 'classic' structural data such as kinematic indicators, measurements of lineations, foliations, etc. Recognition of a syndepositional phase of deformation is based on observations such as the existence and extent of intraformational fold and fault patterns, block rotations, thickness variations, and local unconformities.

The cross-sectional view provided by the map (Fig. 3) allows for the recognition of intraformational structural features such as bedding orientations that deviate from the overall strike. Similarly, aerial and satellite photographs can be used to determine the existence and extent of intraformational fold and fault patterns, block rotations, thickness variations, and local unconformities. Together with sufficiently detailed field checks, in particular on the orientation of bedding versus fault planes, aerial photograph analysis forms an important component of the structural analysis of the early deformation in this study. This kind of analysis resembles the analysis of seismic sections in oil exploration, but with a much wider possibility for field checks.

### *3.3.1. Structure of the Buck Ridge volcano-sedimentary complex*

The offsets along the array of ∼2–4 km spaced northeast-striking faults that cut the BR-vsc, are particularly well visible in the felsic volcanic and volcaniclastic rocks, and the lower part of the silicified sediments of the BRC. The rock succession has been displaced sinistrally along these faults.

The offset along the faults is largest (up to ∼1.3 km) in the bimodal volcanic part of the rock succession, and decreases stratigraphically upwards in the BR-vsc (e.g. Fig. 8) to 0 in the uppermost unit of the BRC. As indicated in Section 3.2.1, the felsic rock succession and the overlying BRC also show significant variations in thickness across the major faults. In the silicified sedimentary rocks of the BRC, the thickness variations of rock units across the faults gradually decrease to 0. The uppermost unit, the well-banded silicified sandstone, has a relatively constant thickness across the faults. The stratigraphically downward increasing offsets along the faults and the corresponding thickness variations across the faults (e.g. Fig. 8) characterise these faults as syndepositional (i.e. as growth faults) that subsequently rotated along with the bedding into their present position. *This being assessed, the faults can now be characterized and described as west-block-down, listric, normal faults*.

In the hanging walls of these normal faults, where the thickness of the rock succession is maximal, the strike of the bedding deflects from the regional ∼E–W into a NW–SE orientation (i.e. implying clockwise rotation up to a maximum of ∼60°). Between 30°52′E and 30°54′E (Fig. 3) a wide rollover anticline is observed. In the footwalls of the faults, the succession shows local unconformities (e.g. Fig. 9).

At both ends of the fault array, the structure is more complex. At the rear of the array, between 30°57′E and 30°59′ E (Fig. 3), the major NE-oriented faults are folded and the internal structure of the rock succession is chaotic. Locally, parts of the succession are southeast-younging (pillow basalts at loc. HV98-165; Figs. 3 and 4). At the front of the fault array, between 30°50′E and 30°51′E, the lower chert units of the BR-vsc show normal faulting. However, the upper chert units in that area form a complex stack of forward (westward) and backward (eastward) thrust and rotated blocks (Figs. 3 and 10). Eastward, these units link up with several units of the BRC (notably the top of the lower chert, the iron-oxide rich sandstone–siltstone interval and the upper, well-banded silicified sandstone, Fig. 9).

At the base of the BR-vsc, about 2 km below the top of the complex, a number of ∼E–W striking, approximately bedding parallel shear zones occur in a dominantly mafic to ultramafic succession (Fig. 3, cf. Dann, de Wit, and King, all three unpublished maps). Where visible, the character of the shear zones is brittle and intensely fractured. The chert layers between the shear zones (the two lowermost chert horizons in Fig. 3) show many compressive features such as minor thrusts with upper-block west displacement and S-shaped, 100-m scale folds with near-vertical fold axes occur along and in the vicinity of the shear zones. Backthrusts rarely occur as well (e.g. at 30°55′E; Fig. 3).

### *3.3.2. Structures within the Granville Syncline*

At 30°54′E, the axis of the Granville Syncline shows a weak culmination (10° plunge to the east at loc. HV98-261), and the BRC can be traced from the southern into the northern limb. In the eastern part of the map area (∼30°58′E; Fig. 3) a reversal of younging direction

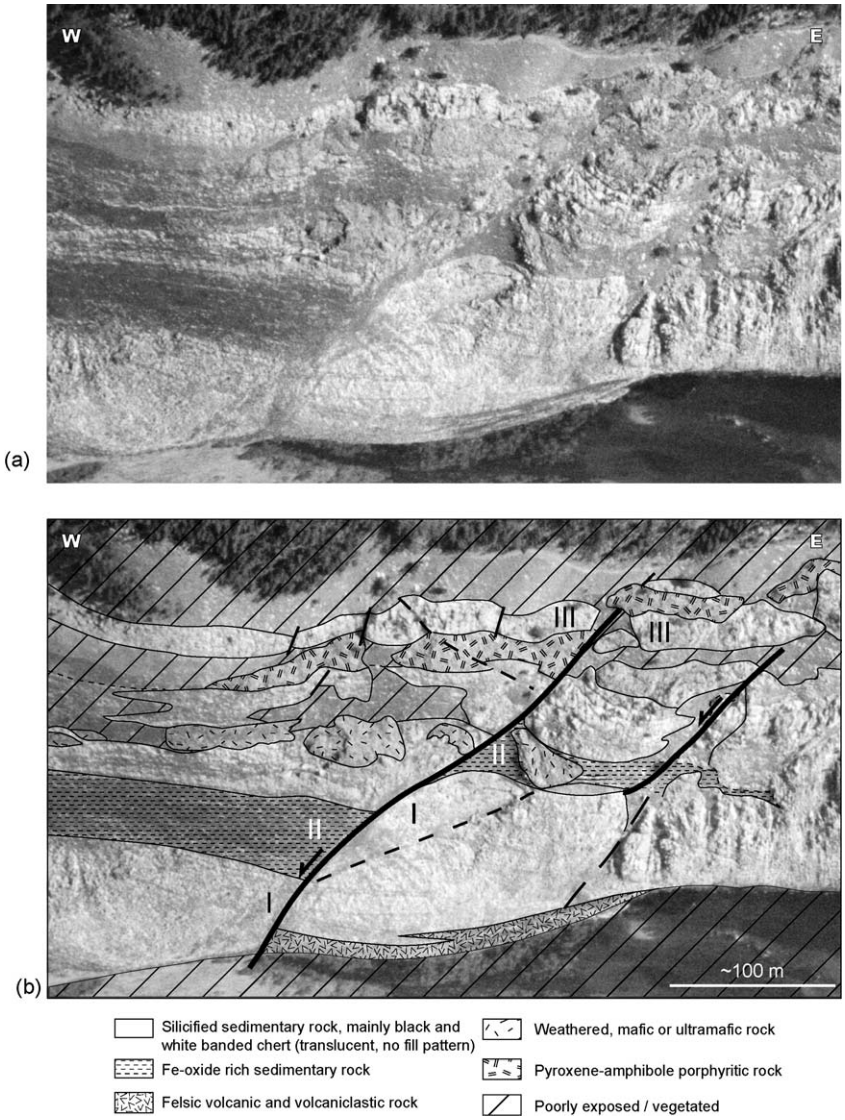


Fig. 8. (a) Oblique aerial photograph of west-block-down normal fault in the sedimentary succession of the BR-vsc, and (b) photograph overlain by field observations and interpretation. Note the thickness difference of the iron-oxide-rich unit (indicated with II) on both sides of the fault, and the upward decrease in offset along the fault. Corresponding units on both sides of the fault have corresponding numbers. Location indicated in Fig. 4.

occurs within the BRC. Between these two locations, en echelon, WNW orientated sinistral faults with associated vertical S-folds are observed. Vertical faults without definite asymmetry are found in the core and along the southern limb within the BRC where they interfere with moderately plunging parasitic folds of the major syncline (e.g. loc. HV98-142 in Figs. 3 and 4).

In the eastern part of the Buck Ridge, structural complications in the southern limb of the syncline have created anomalous contacts between mafic deposits of the Kromberg Formation and the BRC (see Section 3.2.3 and Fig. 7).

## 4. Interpretation and discussion

### *4.1. Stratigraphic architecture and environment of deposition of the BR-vsc*

The dominantly mafic to ultramafic lower part of the BR-vsc is relatively poorly exposed, and consequently indications for the environment of deposition are sparse. The widespread occurrence of pillow basalts and chert with cross-bedding indicates subaqueous deposition for parts of the succession. Upwards, the nature of the volcanism changes to bimodal. Flow banding and

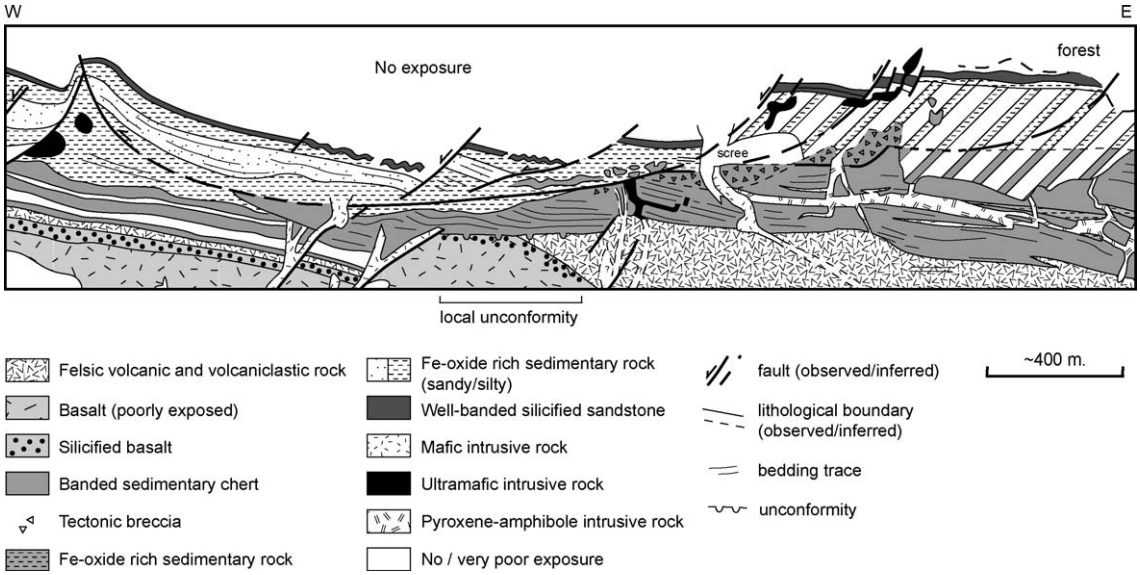


Fig. 9. Gravitational collapse of the upper sedimentary units of the BR-vsc. Location indicated in Fig. 4.

rare columnar jointing in the quartz-plagioclase porphyritic rocks suggest shallow intrusive or extrusive volcanism. The flow-banded felsic rocks are interpreted as lava flows, but most of the quartz-plagioclase porphyritic rocks are massive, and it is difficult to distinguish whether they originated as extrusive or shallow intrusive rocks. In the top of the succession, layers of volcaniclastic rocks and conglomerates indicate (local) erosion and transport of volcanic material. Rare (reworked) accretionary lapilli in the volcaniclastic deposits indicate that volcanism was occasionally explosive. The well-banded silicified sedimentary rocks at the top of the BR-vsc are interpreted as littoral sandstones. They indicate a slight deepening, with respect to the shallow water to subaerial conditions during deposition of lower sedimentary and extrusive volcanic units of the BR-vsc (de Vries, 2004; Nijman and de Vries, 2004; de Vries et al., in preparation). The thickness variations that are characteristic for the stratigraphic architecture of the BR-vsc are not related to abrupt changes in the environment, but are due to the formation of accommodation space by the controlling faults.

### 4.2. Timing of events

The temporal relationship between the intrusive bodies and the lavas of the BR-vsc was established by U–Pb SHRIMP dating. One of the massive felsic intrusions (LV01-113) and a lava flow (LV01-23) in the top of the BR-vsc are both 3451 ± 5 Ma old (Fig. 5a and b), indicating that the extrusive felsic volcanics and the major felsic intrusions in the BR-vsc were broadly contemporaneous. Felsic volcanic rocks on the north limb of the Granville Syncline were dated at 3448 ± 5 Ma (sample ISO99-9; Fig. 5d). An age in the same range, 3452 ± 3 Ma, was obtained for a dacitic tuff from the lowermost part of the felsic unit by Byerly et al. (1996) (sample SA351-2; Table 3). Previously, the same sample had been dated with Pb–Pb evaporation at 3445 ± 3 Ma (Kröner et al., 1991; Table 3). An earlier date, obtained by Armstrong et al. (1990) for a dacite to dacite–andesite composite sample from the massive felsic unit (3445 ± 8 Ma), is within error of the three new dates (sample BSV30/86; Table 3). Hence, the intrusive and extrusive rocks of the felsic complex are approximately contemporaneous, and constrained by a maximum interval of deposition/crystallisation of ~13 Ma. Only one age is available for the volcano-sedimentary succession that overlies the felsic lavas and intrusives of the Hooggenoeg Formation. Kröner et al. (1991) dated a sample from the volcaniclastic top of the felsic volcanic zone or the base of the overlying silicified sedimentary succession of the BR-vsc by Pb–Pb evaporation. Three zircons from a dacitic tuffaceous sandstone in this unit yielded a mean Pb–Pb date of 3416 ± 5 Ma (sample MW64; Table 3). Considering the fact that this Pb–Pb date does not give any information on the concordancy of the data, it has to be regarded as a minimum date. The maximum time span for the extension event is therefore ~35 Ma. The pyroxene-amphibole porphyritic rock that intruded the BR-vsc is ~200 Ma younger than the complex itself. Its age of 3228 ± 3 Ma (Fig. 5c) suggests that the intrusion

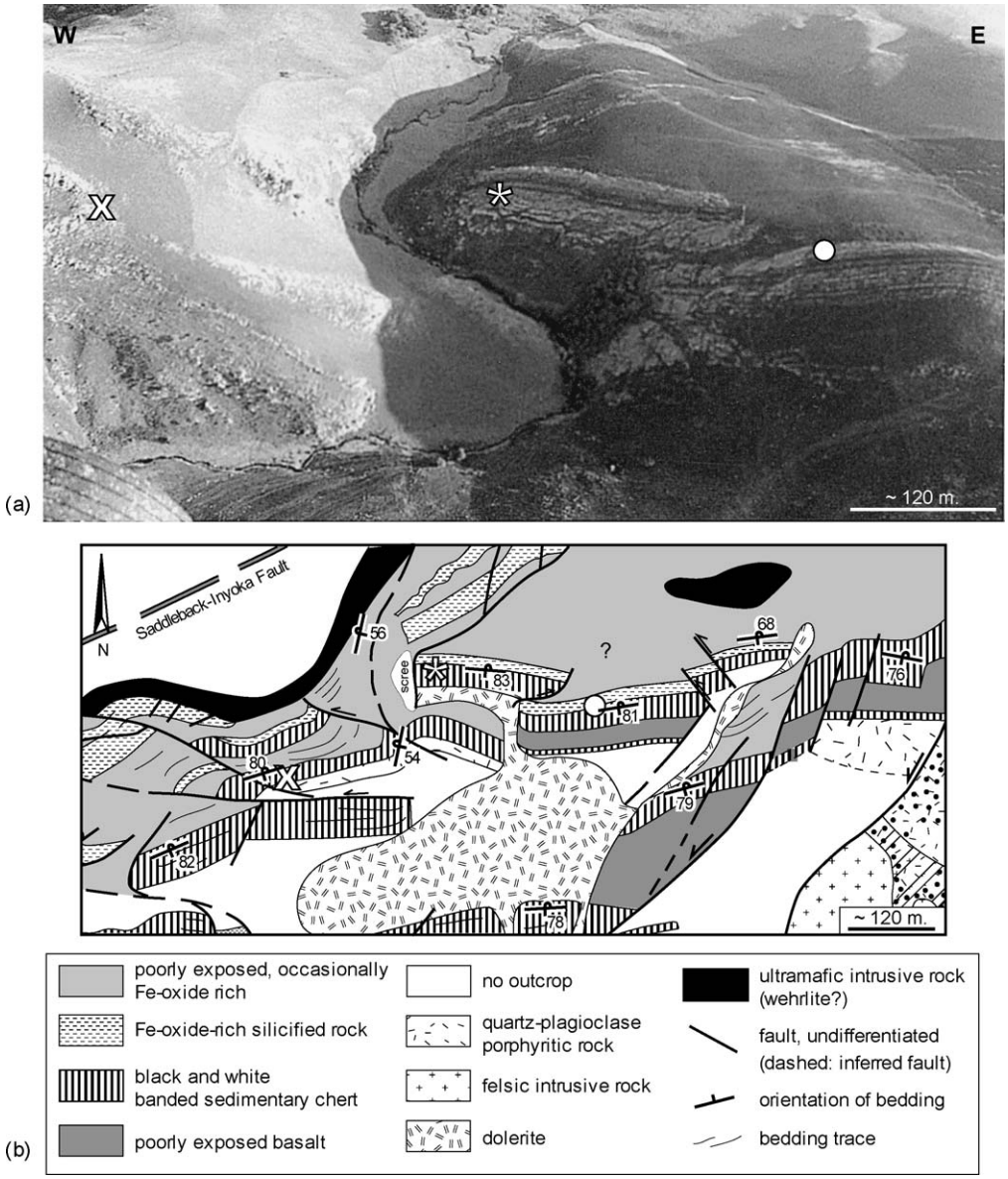


Fig. 10. (a) Oblique aerial photograph of thrust structures in the top of the BR-vsc in the western part of the area. (b) Geological map of approximately the same area as shown in 'a'. Symbols indicate corresponding locations in 'a' and 'b'. Location indicated in Fig. 4.

was related to the phase of igneous activity that also gave rise to the Kaap Valley Pluton, which was dated at 3227 ± 1 Ma (Kamo and Davis, 1994).

### 4.3. Structural control on the deposition of the BR-vsc

#### 4.3.1. Growth-fault control

Unravelling the earliest phase of deformation that affected the BR-vsc in the Barberton Greenstone Belt is essential for interpreting the dynamics of formation of this early Archaean basin (cf. Nijman and de Vries, 2004). For the BR-vsc, syndepositional normal faulting, and therefore extension, is interpreted as the dominant structural control. Direct influence of the faulting on deposition is visible in both the distribution of the felsic rocks in the complex and in the sedimentary facies, for instance in the eastern part of the area, where coarse clastic deposits are concentrated along the down-thrown sides of the normal faults (Fig. 3). At depth, the traces of the normal faults are either poorly exposed or obscured by felsic intrusive bodies. However, from the shape and

Table 3
Origin and age of zircon dating samples from the BR-vsc and the area immediately north of the BR-vsc on the northern limb of the Onverwacht Bend in the southern Barberton Greenstone Belt

| Sample number | Age (Ma) | Latitude | Longitude | Reference |
|---|---|---|---|---|
| LV01-113 | 3451 ± 5 | S 25°56.15′ | E 30°53.37′ | This study[a] |
| LV01-23 | 3451 ± 5 | S 25°56.11′ | E 30°53.44′ | This study[a] |
| SV01-3 | 3228 ± 3 | S 25°55.23′ | E 30°53.02′ | This study[a] |
| ISO99-9 | 3448 ± 5 | S 25°54.50′ | E 30°53.57′ | This study[a] |
| SA351-2 | 3452 ± 3 | S 25°56.7′ | E 30°43.7′ | Byerly et al. (1996)[a] |
| SA351-2 | 3445 ± 3 | S 25°56.7′ | E 30°43.7′ | Kröner et al. (1991)[b] |
| BSV 30/86 | 3445 ± 8 | Composite sample | | Armstrong et al. (1990)[a] |
| MW64 | 3416 ± 5 | S 25°55.5′ | E 30°51.6′ | Kröner et al. (1991)[b] |

SHRIMP dating for this study was done at Australian National University in Canberra, Australia, locations indicated in Fig. 4, details in Fig. 5a–d, and Appendix A.
[a] Dating method: SHRIMP zircon U–Pb.
[b] Dating method: Pb–Pb evaporation.

spacing of the intrusive bodies, the distribution of felsic and mafic volcanic rocks in the BR-vsc, and the preserved fragments of the fault traces, it is interpreted that the largest faults merge listrically into the shear zones along the base of the BR-vsc (Fig. 3). In such an interpretation, the shear zones at the base of and just below the level of the felsic intrusions would have acted as the zone of detachment for the accommodation of block displacements along the array of normal faults. Vergence of the folds and the upper-block west displacement along minor thrust faults in the vicinity of the shear zones, are synthetic with the west-block-down movement of the listric normal faults. The shear zones also mark the southern limit of fault block rotations and other intraformational deformation in the area. The progressive tilt of the volcanic succession in the hanging walls of the faults is a well-known feature in synsedimentary collapse structures and often results in rollover anticline formation (e.g. Mandl and Crans, 1981; Mauduit and Brun, 1998), a phenomenon that was also observed in the western part of the BR-vsc. In the eastern part of the area (at the rear of the fault array), progressive gravitational collapse led to folding of the fault planes, chaotic deformation of the stratigraphic succession and oversteepening of the easternmost rollover anticlines. The latter resulted in local south-younging of the stratigraphic succession. Hence, the local overturning of the stratigraphic succession in this area is interpreted to be a direct result of gravitational collapse, and is therefore considered to have been contemporaneous with deposition of the felsic rocks in the upper Hooggenoeg Formation. Probably, the already complex structures at the rear of the fault array were subsequently deformed further as a result of space problems due to trondhjemite emplacement, or during formation of the Onverwacht Bend. The compressive structures in the western part of the area are interpreted to be due to thrusting in the toe of the normal fault array (e.g. Mandl and Crans, 1981). The upper part of the sedimentary succession in that area was affected by late-stage superficial gravitational collapse (Fig. 9). The massive felsic rocks have intruded along the major normal faults (Fig. 3). Dating (this study) shows that they were broadly contemporaneous with the extrusive felsic rocks in the top of the BR-vsc (Fig. 5a and b). Their texture (porphyritic, with a high percentage of fine-grained groundmass) shows that they solidified at shallow depth. Hence, the accommodation space created by the extension was not only filled by sediments but also by intrusive and extrusive rocks. Extension also created space, especially in the hanging walls, which were bent by rotation, for the formation of swarms of quartz-plagioclase porphyritic dykes and black chert veins.

#### 4.3.2. Compression versus extension

Observations of extensional deformation in the Barberton Greenstone Belt around ~3.4 Ga are not new. Extensional faulting in the uppermost part of the felsic volcanics and the lowermost part of the BRC was recognised previously (Viljoen and Viljoen, 1969; Lowe and Fisher Worrell, 1999), but this was explained as local faulting, perhaps related to cooling and subsidence of an underlying felsic intrusion (Lowe et al., 1999). For the area slightly northeast of the present study area (de Wit, 1982) already introduced the concept of gravity tectonics based on observations in the upper Onverwacht and Fig Tree Groups. He described large-scale mass transport down an unstable paleo-slope into deeper parts of the basin. The subhorizontal thrust or glide planes in that area were explained as either mass transportation during a later phase in a direction opposite to that of the gravitational mass transport, or contemporaneous nappe formation in the same direction, which caused gravita-

tional instability in its front. However, in later articles about the deformation history of the southern Barberton Greenstone Belt the idea of gravitational deformation, either prior to a phase of thrusting or contemporaneous with thrusting, has no longer been considered. Gravitational deformation and the formation of extensional arrays of faults in one area often leads to compressive structures along the sole and in the toe region of the normal fault or fault array (e.g. Mandl and Crans, 1981). The observations near the base of the felsic complex of the upper Hooggenoeg Formation can be explained in this way. Lowe et al. (1985, 1999) and Lowe and Byerly (1999b) described a zone of shearing, intrusion and rotated mafic blocks in the upper part of the Hooggenoeg Formation, which they termed the Geluk disturbed zone. Since the fault forming the lower contact of the zone was not observed to cut the units overlying the felsic zone (or member H6; Lowe et al., 1999; Fig. 2), this deformation was considered to be pre-BRC (member K1 of Lowe et al., 1999; Fig. 2). The Geluk Fault of Lowe et al. (1999) coincides for the major part with the inferred detachment zone of the growth-fault model of this study. In the western part of the area the Geluk Fault coincides with the combined traces of growth faults and detachment faults in this study. Large, detached and rotated masses of basaltic and komatiitic volcanic rock at lower stratigraphic levels were described to be surrounded by the felsic intrusive body of H6 (Lowe et al., 1985, 1999; Lowe and Byerly, 1999b). In the present model, these are interpreted as *in situ* basalts alternating with bedding-parallel felsic porphyritic rocks, which systematically rotated along normal faults and were subsequently intruded by felsic magma. Therefore, observations of compressive structures in the study area by other authors do not necessarily contradict the extension model proposed in this study. De Ronde and de Wit (1994) regard the earliest phase of regional deformation (D1) to be compressional. This phase was timed at 3445–3416 Ma, based on the ages of felsic intrusives (ages listed in de Ronde and de Wit, 1994) that were interpreted to have been syntectonic. D1 deformation included the formation of recumbent nappes, downward facing sequences (de Wit, 1982; de Wit et al., 1987a) and the emplacement of ophiolite allochthons (de Wit et al., 1987b).

New field and geochronological data have improved the timing of events during and just after deposition of the Hooggenoeg Formation. This leads to a different interpretation of previous observations; some observations thought to belong to different phases of deformation are now interpreted to be contemporaneous with deposition of the BR-vsc. De Wit et al. (1987a) argued that the felsic intrusive rocks of the upper Hooggenoeg Formation were emplaced during thrusting at or near the boundary between the Onverwacht pillow lava-chert sequence and a cover of Fig Tree-like shales. The emplacement postdated an early period of deformation, which included local overturning of Onverwacht stratigraphy. Plunging to vertical folding, which resulted in reversal of younging of parts of the stratigraphic succession along the lower contact of the felsic intrusion on the northern limb of the Onverwacht Bend, has been explained as postdating or accompanying the felsic intrusion (de Wit et al., 1987a). Based on the new evidence presented here, it is likely however, that both folding and local overturning of stratigraphy were the direct effect of large-scale normal faulting during deposition of the felsic volcanic succession in the top of the Hooggenoeg Formation. U–Pb SHRIMP dating has shown that the felsic extrusives near the top of the formation were approximately contemporaneous with emplacement of the felsic intrusions in the upper Hooggenoeg Formation. Hence, the local folding and overturning of small parts of the Onverwacht (Hooggenoeg) stratigraphic column, and the emplacement of felsic intrusions may have occurred during a single, early phase of deformation, rather than during two or three separate phases.

### *4.4. Post-BR-vsc deformation: implications for stratigraphy*

The existence of the Granville Syncline is corroborated by the dating of sample ISO99-9 at $3448 \pm 5$ Ma, from the north limb of the syncline. It implies that the BR-vsc reappears in the area north of the Buck Ridge. This may have important implications for the stratigraphic interpretation of the folded and undated chert units further to the north, such as the Umsoli Chert (Heinrichs, 1984). The folding immediately north of the Buck Ridge is interpreted to belong to the D2 phase of NW–SE regional compression, which was already known from the central part of the Barberton Greenstone Belt (Table 1), and dated (de Ronde et al., 1991; Kamo and Davis, 1994; de Ronde and de Wit, 1994) at ~3230 Ma. The syncline was subsequently affected by sinistral strike slip creating en echelon faults and vertical folds in particular along the northern limb (D3: <3226 Ma). D3 also resulted in the formation of the Onverwacht Bend. Our observations fit with the recognition of reversals of younging direction and fold closures north of the BRC by de Wit (1982). Furthermore, several authors have suggested that the uppermost ultramafic lavas of the Onverwacht Group and the overlying Fig Tree sedimentary rocks are repeated in a series of thrust

and fold nappes (de Wit, 1982; de Wit et al., 1983; Lowe et al., 1985). The post-BR-vsc (D2) folding that resulted in the formation of the Granville Syncline is interpreted to have been indirectly responsible for the missing top of the BR-vsc between ∼30°57′E and 30°58′E (Figs. 3 and 7). Previously, this structure was explained as a crater that had resulted from violent, hydromagmatic explosions, and was filled with mafic lapillistone and lapilli tuff (Ransom et al., 1999). The straight, bedding-perpendicular sides of the structure, visible on aerial photographs, are faults (Fig. 7a). The structure is explained as being due to dip-slip gravitational collapse of part of the southern limb of the Granville Syncline (Fig. 7b), in a way comparable to that of the classic examples of the Asmari Limestone of Iran (Harrison and Falcon, 1936). This accounts for the local disappearance of the top of the BRC, and juxtaposition of Kromberg Formation mafic lapilli and lower sedimentary units of the BR-vsc between ∼30°57′E and 30°58′E (Figs. 3 and 7). Alternatively, the rocks may have been repeated along a fault surface with the Granville Syncline representing an overfold or nappe (formed at ∼3.2 Ga). This may be linked to movement along the Saddleback-Inyoka Fault.

### 4.5. Comparison with other Archaean examples

The first recognised deformation structures in several greenstone belts of the Pilbara (Australia) are ∼3.47–3.46 Ga. These include tilting of the Coonterunah Group (Buick et al., 1995; Green et al., 2000), and formation of arrays of syndepositional listric normal faults (Zegers et al., 1996; Nijman et al., 1998; de Vries et al., 2006). The latter are comparable to and approximately contemporaneous with the extensional structures in the upper Hooggenoeg Formation. Key structures are brittle extensional faults that crosscut the stratigraphic succession and at their sole merge into highly altered bedding-parallel shear zones, usually located in ultramafic units. The recognition of an early extensional phase of deformation in the Barberton Greenstone Belt makes the already very comparable tectonic histories of the Kaapvaal and Pilbara Cratons (Zegers et al., 1998) even more similar.

## 5. Conclusions

Normal growth faulting controlled the deposition of the 3.45–3.41 Ga Buck Ridge volcano-sedimentary complex (BR-vsc). The growth-fault model accounts for previously unexplained structural observations, such as intraformational block rotations in the top of the Hooggenoeg Formation, and for the concurrence of D1 extensional and compressional structures. The BR-vsc is a bimodal volcanic complex, with felsic volcanism becoming increasingly dominant upward. The top of the complex is formed by a silicified, partly volcaniclastic, sedimentary succession; the Buck Ridge Chert. The BR-vsc was intruded by broadly contemporaneous, shallow felsic porphyritic rocks, which follow the traces of the normal faults, thereby obscuring many of the diagnostic features of the faults. Extension created accommodation space, not only for sediments, but also for bimodal volcanic rocks, for the intrusive emplacement of felsic sills. Approximately bedding-perpendicular felsic and mafic dykes, and black chert vein systems developed along fractures that were caused by stretching in the fold blocks due to tilt along the growth faults.

## Acknowledgements

STdV and WN thank Prof. M.J. de Wit for inviting them to work on the enigmatic geology of the upper Hooggenoeg Formation, for his help to start up the project, and for providing logistic support from the University of Cape Town. STdV and WN are grateful to Dr. J.C. Dann for introducing them in the geology of the southern Barberton Greenstone Belt. We gratefully acknowledge access to the unpublished maps of M.J. de Wit, J.C. Dann and V. King. Students O. Houtzager and K.L. Louzada contributed to this article with their MSc theses on parts of the BR-vsc. Dr. M.J. van Bergen is thanked for the advice on the volcanology. U–Pb SHRIMP dating was carried out by the first author at the SHRIMP-RG of the Research School for Earth Sciences at Australian National University in Canberra (Australia), in cooperation with the third author. This dating was financed with contributions from the Geodynamical Research Institute (GOI) and The Netherlands Organization for Scientific Research (NWO, grant R 75-394). The Foundation Dr. Schürmannfonds supported the fieldwork as part of the Earth's Earliest Basins-project with grants 1998/14, 1999/14, 2001/14 and 2002/10. Comments on earlier versions of this manuscript by Prof. P.L. de Boer, Prof. M.J. de Wit and Dr. C.E.J. de Ronde are gratefully acknowledged. Two anonymous reviewers are thanked for their comments and suggestions that helped to improve this article.

## Appendix A

### A.1. Analytical technique

Zircons were separated from 8 to 9 kg rock samples at the mineral separation laboratory of the Free University

in Amsterdam. The samples were crushed and ground with a rock splitter, jaw crusher and disk mill to a size of <500 μm. The samples were then sieved to obtain a fraction smaller than 250 μm. Light particles smaller than 32 μm were removed. Zircons were separated from the remaining fraction using standard heavy liquid and magnetic separation techniques. At ANU, the hand-picked zircons, together with the zircon standards SL13 and FC1, were mounted in epoxy resin and polished. Spots for analyses were selected using transmitted and reflected light microscopy images, as well as SEM cathodoluminescence images of the mounted zircons. The analyses were carried out on the SHRIMP-RG of the Research School for Earth Sciences at the Australian National University in Canberra. The SHRIMP data were collected and reduced in a manner similar to that described by Williams (1998, and references therein), using the SQUID Excel Macro of Ludwig (2000). U/Pb ratios in the unknown samples were normalised to a $^{206}Pb/^{238}U$ value of 0.1859, equivalent to and age of 1099.1 Ma (Paces and Miller, 1993) for zircon standard FC1. U and Th concentrations were determined relative to those measured in the SL13 standard (Claoué-Long et al., 1995). Corrections for common lead were made using the measured $^{204}Pb/^{206}Pb$ ratios and the appropriate model Pb compositions from Stacey and Kramers (1975). Uncertainties in the SHRIMP results (tables and plots) are reported at the 1 sigma level, whilst final ages are reported as weighted means with 95% confidence limits. Statistical analyses and age calculations were done using the software Isoplot/Ex Version 2.00 (Ludwig, 1999).

### A.2. Results

#### A.2.1. LV01-23

The zircons from this flow-banded, quartz-plagioclase-bearing porphyritic rock are pink, generally 110–130 μm long, and mostly stubby. They are magmatic, with well-developed compositional zoning. Twenty-eight spots were analysed on 25 grains from this sample (Table B.1, Appendix B). Most of the analyses show disturbance due to recent as well as older Pb-loss and are discordant. Only five analyses are concordant within error. The age based on these five analyses has a large error and a very large MSWD. Rejecting the youngest one (20.1), assuming it has suffered Pb-loss like most other zircons in this sample, significantly improves the error and MSWD. The four remaining analyses (1.1, 7.1, 15.1 and 16.2) combine to define a weighted mean $^{207}Pb/^{206}Pb$ age of 3451 ± 5 Ma (MSWD = 0.71; probability = 0.55).

#### A.2.2. LV01-113

The zircons from this plagioclase and quartz-bearing intrusive rock are pink, 70–190 μm in length, subhedral to euhedral, with magmatic compositional zoning preserved. Many zircons are fractured. Twenty-nine analyses were made on 22 different zircons (Table B.2, Appendix B). Analysis 1.1 is excluded from the diagrams and calculations because analytical problems occurred during measurement. The overall trend of the data indicates non-recent Pb-loss. Duplicate measurements on several zircons show that this is a real trend and not an artefact resulting from analytical problems. Hence, the resulting $^{207}Pb/^{206}Pb$ ages must be regarded as minimum ages, and determination of an absolute age by calculating a regression line is statistically impossible. Six analyses together (1.2, 11.2, 15.1–17.1 and 20.1) define a mean $^{207}Pb/^{206}Pb$ age of 3451 ± 5 Ma (MSWD = 1.2; probability = 0.30).

#### A.2.3. SV01-03

Zircons from this altered, pyroxene-amphibole-bearing intrusive rock are pink, very clear (translucent) and show little fracturing. Most of the crystals are highly elongated, generally 110–180 μm in length, euhedral and compositionally zoned. The sample contains many fragments of zircons. Twenty grains were analysed with one single spot per grain (Table B.3, Appendix B). Apart from one discordant analysis (8.1, Fig. 5c), all data plot in one group, which gives a weighted mean $^{207}Pb/^{206}Pb$ age of 3228 ± 3 Ma (MSWD = 0.71; probability = 0.80).

#### A.2.4. ISO99-9

The zircons from this quartz-plagioclase-bearing porphyritic rock are generally small (70–135 μm), stubby, pink and vary in shape from anhedral to euhedral. The cathodoluminescence images of these zircons show that they are zoned. Twenty-five grains were analysed with one spot per grain (Table B.4, Appendix B). Most of the data are discordant, and they are clearly scattered. Because there are no systematic differences in shape, size or other optical properties of the zircons, there is no reason to assume that the scatter in the data is due to different populations of zircons. No single date can be calculated, but combining the oldest group of data from zircons, which appear to be homogeneous (11 analyses: 1, 2, 5, 6, 8–10, 12, 17, 22 and 24), results in a mean $^{207}Pb/^{206}Pb$ age of 3448 ± 5 Ma. This is the best estimate of the age of crystallisation of the rock. The scatter in the data may be the consequence of Pb-loss soon after crystallisation, causing a Pb-loss discordia parallel to the concordia curve, overprinted by recent Pb-loss. In this case, the calculated weighted mean $^{207}Pb/^{206}Pb$ age

should be regarded as a minimum age for the sample. A second possibility for the spread in the data is that the zircons contain inherited cores and younger rims. The younger ages tend to be from analyses closer to the rim of the zircons, while the older ones are mostly from closer to the centre. Although there are no obvious cores visible on the cathodoluminescence images of the zircons, the inherited grains or cores may look the same and have similar chemistry to the magmatic rims if they come from the same magmatic system. The relatively narrow spread in the data indicates that the inheritance would have been from a source (or sources) not much older than the host rock. If this is indeed a real core/rim relationship, the calculated weighted mean $^{207}Pb/^{206}Pb$ age represents a maximum age for the sample. An alternative option for the fact that the younger ages tend to be near the rims of the zircons is that the Pb-loss is through diffusion, with the margins more affected than the interiors, giving the former younger apparent ages. However, the apparent core-rim relationship observed in the zircons from sample ISO99-9 could just be fortuitous, the data are not sufficient to really prove such a trend, and therefore it is impossible to confirm or reject the last two options. In any case, neither of the above options, if they were true, would shift the age of sample ISO99-9 to younger than ~3441 Ma, so the interpretation of this sample in the text (Section 4.4) would not significantly change.

## Appendix B. Supplementary data

Supplementary data associated with this article can be found, in the online version, at doi:10.1016/j.precamres.2006.04.005.

## References


Armstrong, R.A., Compston, W., de Wit, M.J., Williams, I.S., 1990. The stratigraphy of the 3.5–3.2 Ga Barberton Greenstone Belt revisited: a single zircon ion microprobe study. Earth Planetary Sci. Lett. 101, 90–106.

Brandl, G., de Wit, M.J., 1997. The Kaapvaal Craton, South Africa. In: de Wit, M.J., Ashwal, L.D. (Eds.), Greenstone Belts. Clarendon Press, Oxford, pp. 581–608.

Buick, R., Thornett, J.R., McNaughton, N.J., Smith, J.B., Barley, M.E., Savage, M., 1995. Record of emergent continental crust ~3.5 billion years ago in the Pilbara craton of Australia. Nature 375, 574–577.

Byerly, G.R., Kröner, A., Lowe, D.R., Todt, W., Walsh, M.M., 1996. Prolonged magmatism and time constraints for sediment deposition in the early Archean Barberton greenstone belt: evidence from the upper Onverwacht and Fig Tree groups. Precambrian Res. 78, 125–138.

Claoué-Long, J.C., Compston, W., Roberts, J., Fanning, C.M., 1995. Two Carboniferous ages: a comparison of SHRIMP zircon dating with conventional zircon ages and $^{40}Ar/^{39}Ar$ analysis, geochronology time scales and global stratigraphic correlation. SEPM Spec. Publ. 54, 3–21.

Dann, J.C., 2000. The 3.5 Ga Komati Formation, Barberton Greenstone Belt, South Africa. Part I. New maps and magmatic architecture. S. Afr. J. Geol. 103, 47–68.

de Ronde, C.E.J., 1991. Structural and geochronological relationships and fluid–rock interaction in the central part of the ~3.2–3.5 Ga Barberton Greenstone Belt, South Africa. PhD thesis. University of Toronto, Canada, 370 pp.

de Ronde, C.E.J., de Wit, M.J., 1994. Tectonic history of the Barberton Greenstone Belt, South Africa: 490 million years of Archean crustal evolution. Tectonics 13, 983–1005.

de Ronde, C.E.J., de Wit, M.J., Spooner, E.T.C., 1994. Early Archean (>3.2 Ga) Fe-oxide-rich, hydrothermal discharge vents in the Barberton greenstone belt, South Africa. Geol. Soc. Am. Bull. 106, 86–104.

de Ronde, C.E.J., Kamo, S.L., 2000. An Archaen arc–arc collisional event: a short-lived (ca. 3 Myr) episode, Weltevreden area, Barberton greenstone belt, South Africa. J. Afr. Earth Sci. 30, 219–248.

de Ronde, C.E.J., Kamo, S., Davis, D.W., de Wit, M.J., Spooner, E.T.C., 1991. Field, geochemical and U–Pb isotopic constraints from hypabyssal felsic intrusions within the Barberton greenstone belt, South Africa: implications for tectonics and the timing of gold mineralization. Precambrian Res. 49, 261–280.

de Vries, S.T., 2004. Early Archaean sedimentary basins: depositional environment and hydrothermal systems. Examples from the Barberton and Coppin Gap Greenstone Belts. Geol. Ultraiectina 244, 160.

de Vries, S.T., Nijman, W., Wijbrans, J.R., Nelson, D.R., 2006. Stratigraphic continuity and early deformation of the central part of the Coppin Gap Greenstone Belt, Pilbara, Western Australia. Precambrian Res. 147, 1–27.

de Vries, S.T., Nijman, W., de Boer, P.L., in preparation. Early Archaean sedimentary rocks of the Buck Ridge (South Africa) and Kittys Gap (Western Australia) volcano-sedimentary complexes.

de Wit, M.J., 1982. Gliding and overthrust nappe tectonics in the Barberton greenstone belt. J. Struct. Geol. 4, 117–136.

de Wit, M.J., 1983. Notes on a preliminary 1:25000 geological map of the southern part of the Barberton greenstone belt. In: Anhaeusser, C.R. (Ed.), Contributions to the Geology of the Barberton Mountain Land. Spec. Publ. Geol. Soc. S. Afr., vol. 9, pp. 185–187 and map.

de Wit, M.J., 1986. Extensional tectonics during the igneous emplacement of the mafic-ultramafic rocks of the Barberton greenstone belt (abstract). Tech. Rep. Lunar Planet. Inst. 86-10, 84–85.

de Wit, M.J., Fripp, R.E.P., Stanistreet, I.G., 1983. Tectonic and stratigraphic implications of new field observations along the southern part of the Barberton greenstone belt. In: Anhaeusser, C.R. (Ed.), Contributions to the Geology of the Barberton Mountain Land. Spec. Publ. Geol. Soc. S. Afr., vol. 9, pp. 21–29.

de Wit, M.J., Armstrong, R., Hart, R.J., Wilson, A.H., 1987a. Felsic igneous rocks within the 3.3 to 3.5 Ga Barberton Greenstone Belt: high crustal level equivalents of the surrounding Tonalite–Trondhjemite terrain, emplaced during thrusting. Tectonics 6, 529–549.

de Wit, M.J., Hart, R.A., Hart, R.J., 1987b. The Jamestown ophiolite complex, Barberton mountain belt: a section through 3.5 Ga oceanic crust. J. Afr. Earth Sci. 6, 681–730.

Green, M.G., Sylvester, P.J., Buick, R., 2000. Growth and recycling of early Archaean continental crust: geochemical evidence from the Coonterunah and Warrawoona Groups, Pilbara Craton, Australia. Tectonophysics 322, 69–88.

Harrison, J.V., Falcon, N.L., 1936. Gravity collapse structures and mountain ranges, as exemplified in south-western Iran. Q. J. Geol. Soc. Lond. 92, 91–102.

Heinrichs, T., 1984. The Umsoli Chert, turbidite testament for a major phreatoplinian event at the Onverwacht/Fig Tree transition (Swaziland Supergroup, Archaean, South Africa). Precambrian Res. 24, 237–283.

Kamo, S.L., Davis, D.W., 1994. Reassessment of Archean crustal development in the Barberton Mountain Land, South Africa, based on U–Pb dating. Tectonics 13, 167–192.

Kisters, A.F.M., Stevens, G., Dziggel, A., Armstrong, R.A., 2003. Extensional detachment faulting and core-complex formation in the southern Barberton granite–greenstone terrain, South Africa: evidence for a 3.2 Ga orogenic collapse. Precambrian Res. 127, 355–378.

Kröner, A., Byerly, G.R., Lowe, D.R., 1991. Chronology of early Archaean granite–greenstone evolution in the Barberton Mountain Land, South Africa, based on precise dating by single zircon evaporation. Earth Planetary Sci. Lett. 103, 41–54.

Lowe, D.R., Byerly, G.R. (Eds.), 1999a. Geologic Evolution of the Barberton Greenstone Belt, South Africa, vol. 329. Geological Society of America Special Paper, 319 pp.

Lowe, D.R., Byerly, G.R., 1999b. Stratigraphy of the west-central part of the Barberton Greenstone Belt, South Africa. In: Lowe, D.R., Byerly, G.R. (Eds.), Geologic Evolution of the Barberton Greenstone Belt, South Africa, vol. 329. Geological Society of America Special Paper, pp. 1–36.

Lowe, D.R., Byerly, G.R., Heubeck, C., 1999. Structural divisions and development of the west-central part of the Barberton Greenstone Belt. In: Lowe, D.R., Byerly, G.R. (Eds.), Geologic Evolution of the Barberton Greenstone Belt, South Africa, vol. 329. Geological Society of America Special Paper, pp. 37–82.

Lowe, D.R., Byerly, G.R., Ransom, B.L., Nocita, B.W., 1985. Stratigraphic and sedimentological evidence bearing on structural repetition in early Archean rocks of the Barberton Greenstone Belt, South Africa. Precambrian Res. 27, 165–186.

Lowe, D.R., Fisher Worrell, G., 1999. Sedimentology, mineralogy, and implications of silicified evaporites in the Kromberg Formation, Barberton Greenstone Belt, South Africa. In: Lowe, D.R., Byerly, G.R. (Eds.), Geologic Evolution of the Barberton Greenstone Belt, South Africa, vol. 329. Geological Society of America Special Paper, pp. 167–188.

Ludwig, K.R., 1999. Isoplot/Ex version 2.00: A Geochronological Toolkit for Microsoft Excel, vol. 1a. Berkeley Geochronological Center Spec. Publ, 46 pp.

Ludwig, K.R., 2000. SQUID 1.00, A User's Manual, vol. 2. Berkeley Geochronology Center Spec. Publ, 17 pp.

Mandl, G., Crans, W., 1981. Gravitational gliding in deltas. In: McClay, K.R., Price, N.J. (Eds.), Thrust and Nappe Tectonics, vol. 6. Geol. Soc. London Spec. Publ., pp. 41–54.

Mauduit, T., Brun, J.-P., 1998. Growth fault/rollover systems: birth, growth, and decay. J. Geophys. Res. 103, 18119–18136.

Nijman, W., de Bruijne, C.H., Valkering, M.E., 1998. Growth fault control of Early Archaean cherts, barite mounds and chert-barite veins, North Pole Dome, Eastern Pilbara, Western Australia. Precambrian Res. 88, 25–52 (re-edition in 1999, Precambrian Res. 95, 247–274).

Nijman, W., de Vries, S.T., 2004. Early Archaean crustal collapse structures and sedimentary basin dynamics. In: Eriksson, P.G., Altermann, W., Nelson, D.R., Mueller, W.U., Catuneanu, O. (Eds.), The Precambrian Earth: Tempos and Events. Developments in Precambrian Geology, vol. 12, pp. 139–155.

Paces, J.B., Miller, J.D., 1993. Precise U–Pb ages of Duluth complex and related mafic intrusions, northeastern Minnesota: geochronological insights into physical, petrogenetic, paleomagnetic, and tectonomagmatic processes associated with the 1.1 Ga midcontinent rift system. J. Geophys. Res. 98, 13997–14013.

Ransom, B., Byerly, G.R., Lowe, D.R., 1999. Subaqueous to subaerial Archean ultramafic phreatomagmatic volcanism, Kromberg Formation, Barberton Greenstone Belt, South Africa. In: Lowe, D.R., Byerly, G.R. (Eds.), Geologic Evolution of the Barberton Greenstone Belt, South Africa, vol. 329. Geological Society of America Special Publication, pp. 151–166.

Smith, A.J., 1981. The geology of the farms Hooggenoeg 731 JT and Avontuur 721 JT, southwestern Barberton greenstone belt. Unpublished BSc thesis. University of Witwatersrand, Johannesburg, South Africa, 26 pp.

Stacey, J.S., Kramers, J.D., 1975. Approximation of terrestrial lead isotope evolution by a two stage model. Earth Planetary Sci. Lett. 26, 207–221.

Viljoen, M.J., Viljoen, R.P., 1969. The geological and geochemical significance of the upper formations of the Onverwacht Group. Upper Mantle Project. Spec. Publ. Geol. Soc. S. Afr. 2, 113–151.

Williams, D.A.C., Furnell, R.G., 1979. Reassessment of part of the Barberton type area, South Africa. Precambrian Res. 9, 325–347.

Williams, I.S., 1998. U–Th–Pb geochronology by ion microprobe. In: McKibben, M.A., Shanks III, W.C., Ridley, W.I. (Eds.), Applications of Microanalytical Techniques to Understanding Mineralizing Processes. Rev. Econ. Geol., vol. 7, pp. 1–35.

Zegers, T.E., de Wit, M.J., Dann, J., White, S.H., 1998. Vaalbara, Earth's oldest assembled continent? A combined structural, geochronologic and paleomagnetic test. Terra Nova 10, 250–259.

Zegers, T.E., White, S.H., de Keijzer, M., Dirks, P., 1996. Extensional structures during deposition of the 3460 Ma Warrawoona Group in the eastern Pilbara Craton, Western Australia. Precambrian Res. 80, 89–105.